Lift at a soft wall

Heather Davies, Delphine Débarre, Claude Verdier, Ralf P Richter, Lionel Bureau

Lift at a soft wall

Heather Davies,[1] Delphine Débarre,[1] Claude Verdier,[1] Ralf P. Richter,[2,3,*] and Lionel Bureau[1,†]

[1] *Univ. Grenoble Alpes, CNRS, LIPhy, 38000 Grenoble, France*
[2] *School of Biomedical Sciences, Faculty of Biological Sciences, School of Physics and Astronomy, Faculty of Mathematics and Physical Sciences, Astbury Centre for Structural Molecular Biology, University of Leeds, Leeds LS2 9JT, UK*
[3] *CIC biomaGUNE, Paseo Miramon 182, 20014 San Sebastian, Spain*

(Dated: November 30, 2017)

We study experimentally the motion of non-deformable microbeads in a linear shear flow close to a wall bearing a thin and soft polymer layer. Combining microfluidics and 3D optical tracking, we observe that the steady-state bead/surface distance increases with the flow strength. Furthermore, we show that such lift is in quantitative agreement with theoretical predictions based on elastohydrodynamics, which attribute the lift to flow-induced deformations of the layer. Thus, this study provides the first experimental evidence of "soft lubrication" at play at small scale, in a system relevant to *e.g.* the physics of blood microcirculation.

Elastohydrodynamics (EHD) is a key concept in soft matter physics [1–3]. The coupling between flow-induced pressure fields and elastic deformations of fluid-immersed objects is at the heart of topics ranging from the rheology of soft colloids [4] to microfluidic particle sorting [5] and contact-free mechanical probe techniques [6]. EHD is also central to biophysical problems such as swimming of micro-organisms [7], lubrication in synovial joints or blood microcirculation [8]. In the latter context, EHD interactions govern the radial migration of circulating blood cells, which underlies vascular processes such as margination [5, 9, 10]: leukocytes and platelets are observed to flow preferentially close to the vessel walls, while softer red blood cells (RBCs) migrate away from them. This gives rise to the so-called cell-free layer, a μm-thick region forming near the vascular walls and depleted of RBCs [11]. This has been characterized *in vitro*, through shear flow experiments studying how RBCs [12] or model vesicles [13] are repelled by a surface. The classical interpretation for the formation of the cell-free layer is that soft RBCs flowing near a surface deform under the fluid shear stress and experience a non-inertial lift force that pushes them away from the wall [14]. Reflecting this, most *in vitro* studies, as well as numerical [15] and theoretical [16] works, consider interactions between a rigid surface and deformable cells, which adopt an asymmetric shape under flow. Such an asymmetry of the flowing objects is pinpointed as the origin of the lift force arising at the low Reynolds numbers typically encountered in microcirculation. *In vivo*, however, blood flow takes place in compliant vessels. In particular, it is well known that the endothelium (the inner part of blood vessels) is lined by a glycocalyx, a thin (100-1000 nm) and soft (Young's modulus of a few tens to hundreds of Pa) layer of polysaccharides bound to the vessel walls and directly exposed to blood flow [17]. While the importance of the glycocalyx on the overall blood microrheology is recognized [17, 18], its quantitative influence on EHD interactions largely remains to be established. More generally, the question

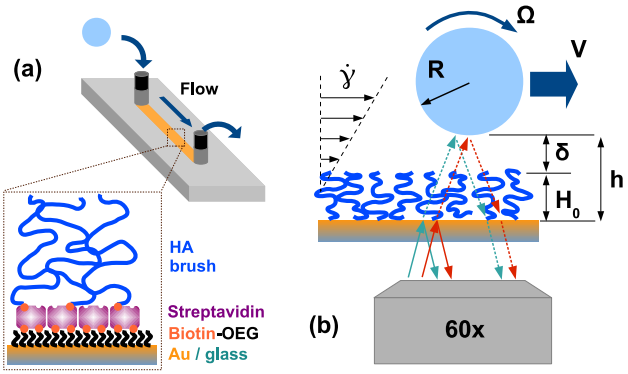

FIG. 1. (a) Parallel plate flow chamber; the bottom surface is functionalized with a HA brush via biotin/streptavidin binding. (b) Bead traveling in a locally uniform shear flow of velocity gradient $\dot{\gamma}$. Dual color RICM is used to monitor its distance h from the substrate and its translation velocity V.

of how a thin deformable layer can contribute to "soft lubrication" and induce lift forces has been addressed theoretically [19–21], but has received limited attention from the experimental standpoint, with a single study investigating at the macroscopic scale how EHD affects the sliding dynamics of cylinders near a soft wall [22]. In this Letter, we report the investigation of the lift experienced by rigid spherical particles flowing in the vicinity of a surface bearing a polymer brush that mimics the glycocalyx. Using microfluidics and three-dimensional (3D) tracking, we provide the first experimental evidence that, under conditions of flow strengths and object sizes relevant to blood circulation, a thin deformable polymer brush gives rise to a sizeable lift force on circulating beads, and that such a lift can be quantitatively described using the theoretical framework developed for soft lubrication.

Experiments were performed at room temperature using a parallel-plate flow chamber (Glycotech, USA) composed of a spacer defining a straight channel (Fig. 1a) of rectangular cross-section (height $H = 0.250$ mm, width

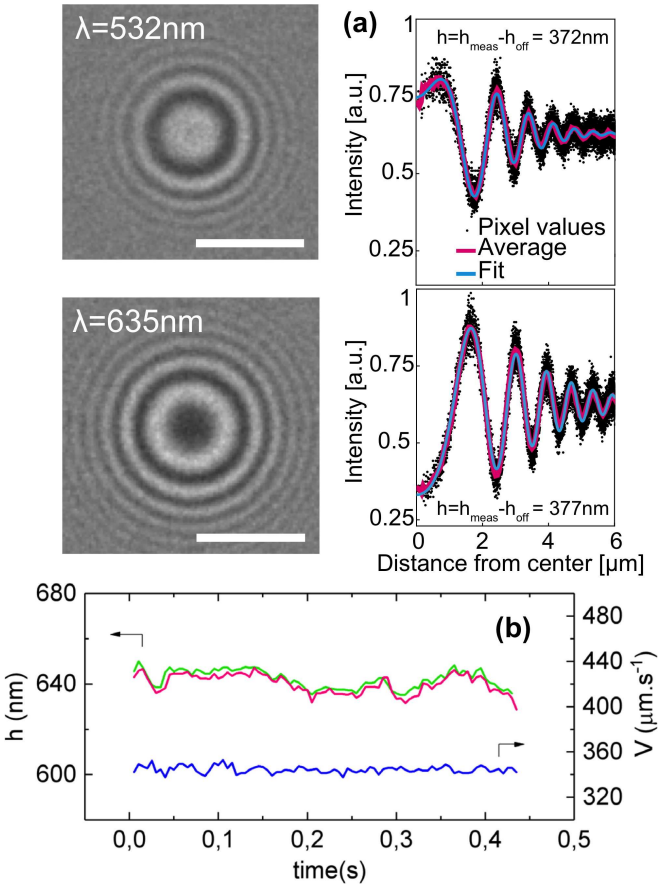

FIG. 2. (a) Left: interference patterns for a bead flowing close to a HA brush (scale bar 5 μm). Right: radial intensity profiles (black dots) are extracted from images, azimuthally averaged (magenta line), and fitted with an optical model (cyan line) to determine $h_{\rm meas}$, from which we compute $h = h_{\rm meas} - h_{\rm off}$, with $h_{\rm off}$ the offset due to the contribution of the gold layer (See section I of Supplemental Material). (b) Time series for h (green: $\lambda = 532$ nm, magenta: $\lambda = 635$ nm) and V (blue), for a bead flowing at $Q = 100\,\mu$L.min^{-1} close to the HA brush.

$W = 2.5$ mm, length $L = 20$ mm), sandwiched between an upper deck with fluid inlet/outlet and a bottom surface consisting of a glass coverslip functionalized with a brush of hyaluronan (HA, the major component of the glycocalyx, see Fig. 1a), as described below. The inlet reservoir contained spherical polystyrene beads of radius $R = 12.5\,\mu$m (Kisker Biotech, Germany) suspended in aqueous buffer (10 mM HEPES, pH 7.4, 150 mM NaCl, 2mM $CaCl_2$, viscosity $\eta \simeq 10^{-3}$ Pa.s and density $\rho \simeq 1000$ kg.m^{-3}), while the outlet was connected to a syringe pump (KDS Legato 110) used in withdraw mode at controlled flow rate in the range $Q = 1-200\,\mu$L.min^{-1}. Beads were pumped into the channel and left to sediment under quiescent conditions onto the bottom surface of the chamber for 5 min, after which their motion under imposed flow rate was monitored optically. 3D tracking was performed by reflection interference contrast microscopy (RICM) using a custom-made setup allowing for simultaneous imaging at two different wavelengths ($\lambda = 532$ and 635 nm). During flow, the fringe patterns produced by interference between the light reflected from the substrate and the surface of the beads were recorded (Fig. 2a) on a CMOS camera (ORCA-Flash4.0 Hamamatsu) at rates of up to 200 frames per second. Bead trajectories were then analyzed offline, using home-written Labview routines, in order to compute for each imposed flow rate: (i) the steady-state vertical distance h between the substrate and the beads, and (ii) the beads' translation velocity V (Fig. 1b and 2b). The absolute value of h was determined unambiguously up to $\sim 1.1\,\mu$m owing to the two-color RICM scheme used [23], with an accuracy of ~ 10 nm (See section I of Supplemental Material). The in-plane displacements of the beads, from which V was computed, were determined by image correlation with an accuracy of $\sim$50 nm.

The surface of the coverslip exposed to the flow was functionalized with a layer of HA, as described in [24, 25]. In brief, a 0.5 nm Ti/5 nm Au layer was evaporated onto the cleaned glass surface. A monolayer of thiols containing end-biotinylated oligo(ethyleneglycol) (bOEG-SH) was grafted onto the gold film. A dense layer of streptavidin was bound to the exposed biotin moieties, and further functionalized with end-biotinylated HA (Fig. 1a). Such a procedure yields HA films that are stably bound to the substrate and adopt a polymer brush conformation [24]. We used HA chains of well-defined molecular weight 840±60 kDa (HA840; Hyalose, USA) [26], which under the incubation conditions used here are expected to yield a brush of thickness 400 ± 40 nm (See section II of Supplemental Material) and low-strain Young's modulus $E \simeq 100$ Pa [24], closely mimicking the thickness and softness of the glycocalyx. On such a surface, we measure a bead height of $h = 375 \pm 10$ nm in the absence of flow. The gravitational force exerted by a bead sedimented on the brush reads:

$$F_{\rm g} = \frac{4\pi R^3}{3} g \Delta\rho \qquad (1)$$

With $g = 9.81$ m.s^{-2} and a density difference of $\Delta\rho = 40$ kg.m^{-3} between the beads and the suspending medium, we compute $F_{\rm g} = 3.2$ pN. From previous mechanical characterization of similar HA brushes [24], we anticipate that such a low force should leave the brush essentially uncompressed. We therefore take $H_0 = 375$ nm as a fair estimate of the unperturbed brush height. As a control surface, we used a plain gold-coated coverslip passivated by a layer of bovine serum albumin to minimize non-specific adhesive bead/surface interactions.

An example time series obtained for h and V of a single bead traveling across the field of view is shown in Fig. 2b. Single bead data were time-averaged, and measurements over ~ 50 different beads were performed under identical flow conditions to obtain the ensemble-averaged values

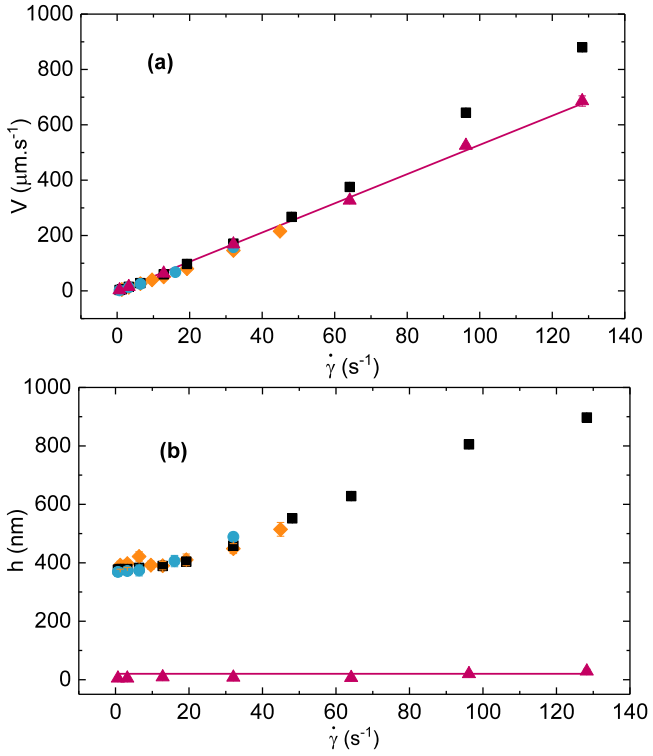

FIG. 3. (a) $V(\dot\gamma)$ measured on control surface (▲), and HA840 brushes (■, ♦, ●, corresponding to three independent measurements). The solid line is the GCB prediction for non-deformable surfaces separated by 20 nm. (b) Experimentally measured $h(\dot\gamma)$ (symbols as in (a)). Solid line indicates the constant value of $z = 20$ nm used in GCB theory. Error bars accounting for standard error and uncertainty on h and V are about the size of the symbols.

of V and h shown respectively in Fig. 3a and 3b as a function of the imposed wall shear rate $\dot\gamma = 6Q/(WH^2)$, on both the gold and HA surfaces.

On the control surface, we observe that V increases linearly with $\dot\gamma$, while h remains small and constant at 15 ± 10 nm over the range of shear rates explored (Fig. 3, triangles). When beads are flowing past a HA brush, their velocity increases linearly with $\dot\gamma$ and h remains close to H_0 at shear rates below $\sim$30 s^{-1}. However, in contrast with the control surface, we see that, for $\dot\gamma >$30 s^{-1}, V grows more than linearly with $\dot\gamma$ while h steadily increases and reaches up to 900 nm at the largest shear rate (Fig. 3). We thus observe a sizeable lift of the beads away from the brush, and now discuss the possible origins of such a phenomenon.

Given the maximum Reynolds number in our experiments, $Re = \dot\gamma R^2\rho/\eta \simeq 10^{-2}$, we first compare the results from the control experiment with the theory developed by Goldman, Cox and Brenner (GCB) to describe the motion of a rigid bead in a shear flow past a non-deformable surface [27]. In the limit where the bead/surface distance $z \ll R$, GCB predict that the bead translation (V) and angular (Ω) velocities (Fig. 1b) depend on z and $\dot\gamma$ as [28]:

$$V = \dot\gamma R \frac{(1+z/R)}{0.7625 - 0.2562\ln(z/R)} \tag{2}$$

$$\Omega = \frac{\dot\gamma}{1.6167 - 0.4474\ln(\delta/R)} \tag{3}$$

Using Eq. (2), we obtain excellent agreement between GCB theory and our data on the control surface when setting $z = 20$ nm (solid lines in Fig. 3), which is quantitatively consistent with the measured values of h. The results of our control experiment therefore match very well the theoretical predictions for a rigid sphere flowing in quasi-contact with a rigid plane.

In order to address the substantial lift of the beads on the HA surface, we first consider whether inertia forces could be at play. Even at the low Re where GCB assumptions apply, it has been shown that an inertial lift force can act on a bead moving close to a wall in a linear shear flow [29, 30]. Cherukat and McLaughlin have computed an expression for this inertial lift force, valid in the limit $z \ll R$ [30]:

$$F_{\rm in} = \rho R^2 V_r^2 I(\Lambda_G, \kappa) \tag{4}$$

where $V_r = V - \dot\gamma(R+z)$ is the difference between the bead velocity and the fluid velocity at the location of the bead center of mass, and $I(\Lambda_G, \kappa)$ is given by

$$\begin{aligned} I =& [1.7669 + 0.2885\kappa - 0.9025\kappa^2 + 0.507625\kappa^3] \\ &- [3.2415/\kappa + 2.6729 + 0.8373\kappa - 0.4683\kappa^2]\Lambda_G \\ &+ [1.8065 + 0.89934\kappa - 1.961\kappa^2 + 1.02161\kappa^3]\Lambda_G^2 \end{aligned} \tag{5}$$

with $\Lambda_G = \dot\gamma(R+z)/V_r$ and $\kappa = R/(R+z)$. Taking $V = 900\,\mu$m.s^{-1}, $\kappa \simeq 1$, and $\dot\gamma = 128$ s^{-1}, we estimate the maximum inertial lift force to be $F_{\rm in} \simeq 1.9$ pN, which is lower than $F_{\rm g}$. Therefore, inertial effects alone cannot induce a significant lift in the range of shear rates explored here, in agreement with our control experiment.

The other mechanism that can lead to lift at low Re is due to elastohydrodynamics, as predicted by theoretical works [19–21]: in the presence of a surface-borne thin and soft layer, its asymmetric elastic deformations (see inset of Fig. 4a) induced by the pressure field in the lubricating fluid are expected to give rise to a lift force ($F_{\rm EHD}$) on a rigid sphere. To test whether elastic deformations of the HA brush could be responsible for our observations, we start from the expression derived by Urzay et al. [21] for $F_{\rm EHD}$:

$$F_{\rm EHD} = \frac{\eta^2 R^2 H_0 {V_s}^2}{(\lambda+2\mu)\delta^3}\left(\frac{48\pi}{125} + \frac{4\pi(19+14\omega)}{25(1+\omega)}\frac{\delta}{R}\right) \tag{6}$$

with η the fluid viscosity, H_0 the layer thickness, λ and μ its Lamé elastic coefficients, δ the distance between

the bead and the top of the layer (see Fig. 4a insert), $V_s = V - \Omega R$, and $\omega = -\Omega R/V$.

At a given shear rate, the steady-state value of δ is set by the balance of vertical forces on a bead:

$$F_{\rm EHD} + F_{\rm in} = F_{\rm g} \tag{7}$$

We further assume that the brush is not penetrated by the shear flow (*i.e.* the no-slip plane of the shear flow is located at the top of the brush) [31]. We thus replace z by δ in Eqs. 2–5, and use GCB results to compute $V_r(\dot\gamma, \delta)$, $V_s(\dot\gamma, \delta)$, and $\omega(\dot\gamma, \delta)$. Doing so, the force balance becomes an equation that depends on δ and contains otherwise only known parameters. The theoretical values for δ can thus be determined at the various imposed $\dot\gamma$ by solving Eq. (7), taking for R, ρ, $\Delta\rho$, η and H_0 the values mentioned earlier in the text. Following the argument given in [20], we take values of the elastic moduli corresponding to conditions where water is free to diffuse over the brush thickness during the passage of a bead (See section III of Supplemental Material). The Young's modulus of the brush is thus set to $E = 100$ Pa, as measured previously [24], and its Poisson ratio to $\nu = 0.3$, a typical drained value for polymer networks [32], from which we get $\lambda + 2\mu = E(1-\nu)/[(1+\nu)(1-2\nu)] \simeq 135$ Pa.

The resulting theoretical predictions for $h(\dot\gamma) = \delta(\dot\gamma) + H_0$ are compared with our data in Fig. 4a. The agreement is found to be very good: as observed experimentally, the theory predicts a lift that stays limited (< 50 nm) at shear rates below 20 s^{-1} and gradually increases up to ~ 500 nm above the brush at larger $\dot\gamma$. Changing the Poisson ratio to $\nu = 0.2$ or 0.4 only marginally affects the agreement (shaded area in Fig. 4a). Eliminating the inertial term in the force balance to account only for EHD (dashed line in Fig. 4a) demonstrates that inertial effects become significant only for $\dot\gamma \geq 50$ s^{-1}, and that EHD alone accounts for about 75% of the lift observed at the highest shear rate. Furthermore, the magnitude of the experimental velocities is comparable to that predicted by GCB at the corresponding $\dot\gamma$ and δ (Fig. 4b). Although the theory tends to overestimate the measured velocities by 10 to 20% at high shear rates, the non-linearity of the $V(\dot\gamma)$ curves is quantitatively captured (Fig. 4b inset). The model being free of adjustable parameters, the overall agreement with experiments is therefore extremely satisfactory. The slight discrepancy on velocities may result from the fact that GCB theory does not account for perturbations of the flow profile induced by the sheared brush, which can be sizeable as shown in recent numerical simulations [33]. This point would require advanced modeling efforts that are beyond the scope of the present study.

In summary, our work shows how a compliant layer affects the near-wall motion of microparticles. Our observations are quantitatively supported by theoretical

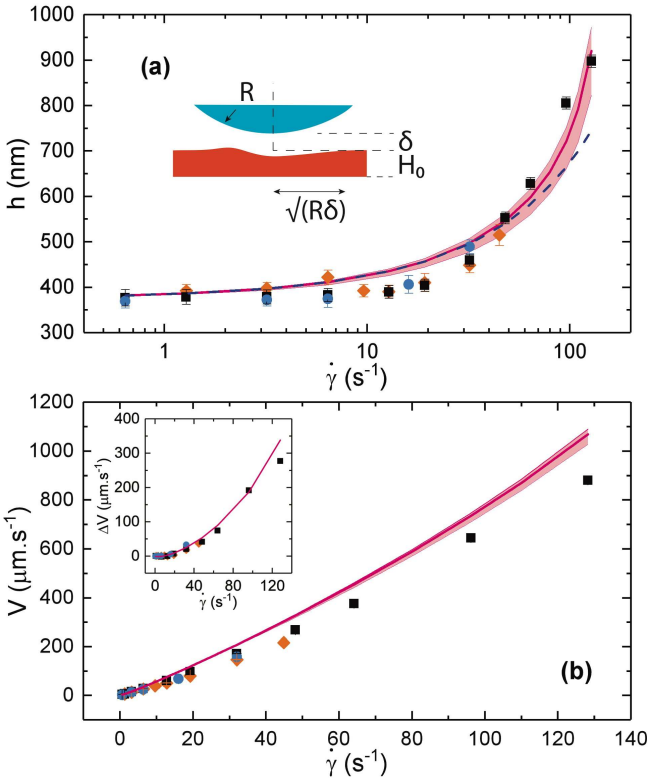

FIG. 4. (a) $h(\dot\gamma)$ data on HA brushes (symbols), and theoretical predictions for $\delta(\dot\gamma) + H_0$ including (red solid line) or neglecting (blue dashed line) inertial lift forces. The shaded area is bound by the predictions for $\nu = 0.2$ (above) and $\nu = 0.4$ (below). Inset: sketch of the asymmetric layer deformation giving rise to EHD lift. Deformation extends laterally over a typical length scale $\sqrt{R\delta}$. (b) Experimental (symbols) and theoretical translation velocities (red line, shaded area computed as above). Inset: measured and predicted deviation from linearity, $\Delta V = V(\dot\gamma) - S\dot\gamma$, with S the slope in the limit of small shear rates.

predictions based on EHD, thus providing direct evidence of soft lubrication at play at small scales. This is likely to have significant influence on the behavior of RBC in blood circulation. Indeed, we compute that the contributions to lubrication forces of wall deformations can be comparable to that of cell deformations. For instance, a RBC ($R \simeq 3\,\mu$m) flowing in plasma ($\eta \simeq 1.5$ mPa.s) under a physiological shear rate $\dot\gamma \simeq 100$ s^{-1} , at a distance $\delta \simeq 0.5\,\mu$m from a μm-thick glycocalyx, would experience a force $F_{\rm EHD} \simeq 0.15$ pN due to glycocalyx deformations (Eq. 6). From a recent study of the drift velocity v_z of RBCs under shear [12], we compute $v_z = \beta\dot\gamma/(R+\delta)^2 \simeq 3\,\mu$m.s^{-1} at the same δ and $\dot\gamma$, with $\beta \simeq 0.36\,\mu$m^3 determined experimentally [12]. This translates into a lift force due to cell deformation $F_{\rm cell} \sim 6\pi\eta R v_z \simeq 0.25$ pN. It thus appears that the contributions of cell and wall deformations to lubrication forces are of comparable magnitude at sub-μm distances from the wall. In conclusion, the present study underlines

the important, yet often overlooked, mechanical role that the soft endothelial glycocalyx is likely to play in regulating cell/wall interactions in blood flow.

We acknowledge the "Emergence" and "AGIR" programs of Université Grenoble Alpes, the Spanish Ministry for Economy and Competiveness (project MAT2014-54867-R, to R.P.R.), the European Research Council (Starting grant 306435, to R.P.R.), the French Agence Nationale de la Recherche (Grant ANR-13-JS08-0002-01, to L.B.), and the Centre National d'Etudes Spatiales (CNES) for funding. We acknowledge the "Prestige" european program and the CNES for fellowships (H.D.). We are grateful to Liliane Coche-Guerente (Department of Molecular Chemistry, Grenoble) for assistance with surface functionalization/characterization, to Luis Yate (CIC biomaGUNE) for gold coatings, and to Gwennou Coupier (LIPhy, Grenoble) for stimulating discussions regarding the lift of RBCs.

* R.Richter@leeds.ac.uk
† lionel.bureau@univ-grenoble-alpes.fr

[1] Y. Wang, G. A. Pilkington, C. Dhong, and J. Frechette, Curr. Opin. Colloid Interface Sci. **27**, 43 (2017).
[2] D. Y. C. Chan, E. Klaseboer, and R. Manica, Soft Matter **5**, 2858 (2009).
[3] Y. Wang, C. Dhong, and J. Frechette, Phys. Rev. Lett. **115**, 248302 (2015).
[4] D. Vlassopoulos and M. Cloitre, Curr. Opin. Colloid Interface Sci. **19**, 561 (2014).
[5] T. M. Geislinger and T. Franke, Adv. Colloid Interface Sci. **208**, 161 (2014).
[6] S. Leroy, A. Steinberger, C. Cottin-Bizonne, F. Restagno, L. Léger, and É. Charlaix, Phys. Rev. Lett. **108**, 264501 (2012).
[7] R. E. Goldstein, E. Lauga, A. I. Pesci, and M. R. E. Proctor, Phys. Rev. Fluids **1**, 073201 (2016).
[8] Z. M. Jin and D. Dowson, Proc. Inst. Mech. Eng. J J. Eng. Tribol. **219**, 367 (2005).
[9] A. Kumar and M. D. Graham, Phys. Rev. Lett. **109**, H318 (2012).
[10] H. Zhao, E. S. G. Shaqfeh, and V. Narsimhan, Phys. Fluids **24**, 011902 (2012).
[11] S. Kim, P. K. Ong, O. Yalcin, M. Intaglietta, and P. C. Johnson, Biorheology **46**, 181 (2009).
[12] X. Grandchamp, G. Coupier, A. Srivastav, C. Minetti, and T. Podgorski, Phys. Rev. Lett. **110**, 554 (2013).
[13] M. Abkarian, C. Lartigue, and A. Viallat, Phys. Rev. Lett. **88**, 876 (2002).
[14] P. M. Vlahovska, T. Podgorski, and C. Misbah, C. R. Physique **10**, 775 (2009).
[15] D. A. Fedosov, B. Caswell, A. S. Popel, and G. E. Karniadakis, Microcirculation **17**, 615 (2010).
[16] P. Olla, Phys. Rev. Lett. **82**, 453 (1999).
[17] T. W. Secomb, R. Hsu, and A. R. Pries, Am. J. Physiol. **274**, H1016 (1998).
[18] E. R. Damiano, B. R. Duling, K. Ley, and T. C. Skalak, J. Fluid Mech. **314**, 163 (1996).
[19] J. Beaucourt, T. Biben, and C. Misbah, Europhys. Lett. **67**, 676 (2004).
[20] J. M. Skotheim and L. Mahadevan, Phys. Fluids **17**, 092101 (2005).
[21] J. Urzay, S. G. Llewellyn Smith, and B. J. Glover, Phys. Fluids **19**, 103106 (2007).
[22] B. Saintyves, T. Jules, T. Salez, and L. Mahadevan, Proc. Natl. Acad. Sci. USA **113**, E8208 (2016).
[23] J. Schilling, K. Sengupta, S. Goennenwein, A. R. Bausch, and E. Sackmann, Phys. Rev. E **69**, 199 (2004).
[24] S. Attili, O. V. Borisov, and R. P. Richter, Biomacromolecules **13**, 1466 (2012).
[25] E. Migliorini, D. Thakar, R. Sadir, T. Pleiner, F. Baleux, H. Lortat-Jacob, L. Coche-Guerente, and R. P. Richter, Biomaterials **35**, 8903 (2014).
[26] F. Bano, S. Banerji, M. Howarth, D. G. Jackson, and R. P. Richter, Sci. Rep. **6**, 34176 (2016).
[27] A. J. Goldman, R. G. Cox, and H. Brenner, Chem. Eng. Sci. **22**, 653 (1967).
[28] Numerical coefficients slightly differ from the original formula by GCB. We have fitted the tabulated numerical values provided in reference [27] and found that the present set of coefficients yields a better agreement than those provided in the original publication.
[29] G. P. Krishnan and D. T. Leighton Jr., Phys. Fluids **7**, 2538 (1995).
[30] P. Cherukat and J. B. Mclaughlin, J. Fluid Mech. **263**, 1 (1994).
[31] The shear flow probably partially penetrates inside the brush. However, the assumption of a no-slip plane at the brush surface is supported by the fact that the experimental $V(\dot{\gamma})$ curves measured with and without brush display a similar slope at low shear rates (Fig. 3a). It suggests that, in both cases, the term that multiplies $\dot{\gamma}R$ in Eq. 2, which depends only on the distance between the bead and the no-slip plane, is of the same magnitude. This implies that, in the presence of the brush, such a distance is comparable to that for the control surface, and should thus be on the order of 10 to 20 nm only, which we neglect with our assumption.
[32] E. Geissler and A. M. Hecht, Macromolecules **13**, 1276 (1980).
[33] S. Biagi, L. Rovigatti, F. Sciortino, and C. Misbah, Sci. Rep. **6**, 2912 (2016).

SUPPLEMENTAL MATERIAL

I Reflection Interference Contrast Microscopy

RICM fringe patterns were fitted with a one-layer optical model accounting for bead curvature and assuming refractive indices of BK7 glass for the substrate, polystyrene for the bead, and water for the intermediate medium (the effect of HA chains on the fluid refractive index is negligible). The contribution of the Ti/Au layer on the glass substrate was treated as a constant offset on the computed distances. We measured this offset $h_{\rm off}$ beforehand by fitting interference patterns of beads in adhesive contact with the bare gold layer, and subtracted it from all subsequently measured heights to compute the actual distance h between the beads and the surface of the gold layer. The accuracy on h was limited by the uncertainty resulting from the offset determination, which, due to minute variations in the gold thickness over the substrates, was ± 10 nm.

II Estimation of the HA brush thickness

In a previous study [24], we have shown that brushes made using HA of molecular weight 1080 kDa (HA1080) have a thickness $h \simeq 550 \pm 50$ nm. From polymer brush theory, we expect the thickness of the polymer layer to scale linearly with the contour length, l_c, of the HA chains. Using $l_c \simeq 2.9\,\mu$m [24] and $l_c \simeq 2.1\,\mu$m [26] estimated respectively for HA1080 and HA840, we thus anticipate the thickness of the HA840 brushes used here to be $h \simeq 400 \pm 40$ nm at comparable HA surface density.

III Estimation of the brush poroelastic time

Following [20], we compute the poroelastic time as $\tau_{\rm p} \sim H_0^2 \eta/(E\zeta^2)$, with E the drained Young's modulus (*i.e.* the modulus measured when fluid is free to flow in or out of the brush), and ζ a typical mesh size which we approximate by the distance between the tethering points of the HA chains. Taking $E \simeq 100$ Pa and $\zeta \simeq 50$ nm, we obtain $\tau_{\rm p} \simeq 5.10^{-4}$ s. This is to be compared with the characteristic probe time in the experiments, given by $\tau_{\rm exp} \sim \sqrt{\delta R}/V$ [20], which we compute from our experimental data to be at least on the order of $\tau_{\rm exp} \simeq 3.10^{-3}$ s. Under such conditions where $\tau_{\rm exp} > \tau_{\rm p}$, the fluid is free to flow over the brush thickness during the passage of a bead. This implies that we should feed the model with the so-called "drained" values of the brush elastic moduli.